

## A Micro-Goniophotometer and the Measurement of Print Gloss

J. S. Arney<sup>▲\*</sup> and Hoon Heo

*Center for Imaging Science, Rochester Institute of Technology, Rochester, New York, USA*

P. G. Anderson<sup>▲</sup>

*Laboratory for Applied Computing, Rochester Institute of Technology, Rochester, New York, USA*

The focus of this report is on the development of an instrument for measuring gloss light. The word “gloss” is intuitively easy to understand, but making an optical measurement that correlates well with the perception of gloss remains an unsolved challenge. The hypothesis behind this project is that both spatial resolution (micro-) and angular resolution (gonio-) are required of an instrument in order to correlate meaningfully with visual perceptions of gloss and also with underlying causes of gloss. Thus, a micro-goniophotometric instrument was developed. The instrument employed plain polarized light to separate bulk, diffuse light from specular light. Specular light was defined instrumentally as the difference between the light captured with a polarizing filter orthogonal to and parallel to the direction of polarization of the incident light. In addition, it was assumed that the instrument must be able to account quantitatively for all of the gloss light from the surface distributed in all directions around the specular (equal/opposite) angle. The instrument developed in this project measures specular and diffuse light as a surface radiance distributed over angle  $\alpha$  from the specular direction in the plane defined by the sample, detector, and illuminator. The orthogonal angle,  $\beta$ , is not scanned. Rather, all of the light distributed in the  $\beta$  direction is integrated at each angle  $\alpha$ . The area under the bidirectional reflectance factor friction, BDRF, generated in this way accounts for all of the specular light distributed over both angles  $\alpha$ , and  $\beta$ . Using this instrument, it was shown that the effects of surface roughness could be differentiated from the effects of variations in refractive index. In addition, the color of the light and the ink were measured and found to vary the amount of specular reflectance by as much as a factor of two. A mechanism is proposed to account for this.

Journal of Imaging Science and Technology, 48: 458–463 (2004)

### Introduction

The word “gloss” is intuitively easy to understand, but making an optical measurement that correlates well with the perception of gloss remains an unsolved challenge. In this report, the term “gloss” is used to describe the visual perception, and the term “specular light” is used to describe light that is reflected at interfaces according to Fresnel’s laws. It is certainly to be anticipated that specular light plays a major role in the visual effects of gloss, but a quantitative relationship between specular light and visual gloss has not been adequately described. The instrument described in the current work does not establish such a connection. However, the instrument was developed to account for all of the specular and diffuse light distributed over both angles and locations. The thesis behind the instrument is that if all of the light can be measured and described, correlates with the many visual effects of gloss should be

extractable from the measurements. This report details the instrument and explores the mechanism of specular reflectance, but correlations with visual gloss have not as yet been thoroughly explored.

Since the long term intent for this instrument is to provide insights into visual gloss, its design was based on literature reports of the nature of visual gloss. Anecdotal experience indicates there are several different properties of gloss that play a role in the overall perception of the quality of a printed image.<sup>1–3</sup> High gloss, for example, is often desirable because one can hold the image in a way that eliminates the gloss, revealing only the printed image. On the other hand, some people prefer a matt finish, even though a matt finish generally has less color saturation. In addition, variations in gloss across the image are highly significant, even if the variations are invisible when the image is viewed in a way that shows no gloss.<sup>4–6</sup> Figure 1(A), for example, shows an electrophotographic image that shows no gloss at all when illuminated and viewed at a 45°/0° geometry. Figure 1(B) shows the same print viewed at 45°/45°, and gloss is easily seen at this geometry. Although one does not intentionally view a print at a geometry that maximizes visual gloss, the mottled appearance of the gloss is found to be objectionable to some viewers and leads to an impression of lower overall image quality. Furthermore, variations in gloss between different printed

Original manuscript received January 8, 2004

▲ IS&T Member

\* ARNEY@cis.rit.edu

©2004, IS&T—The Society for Imaging Science and Technology

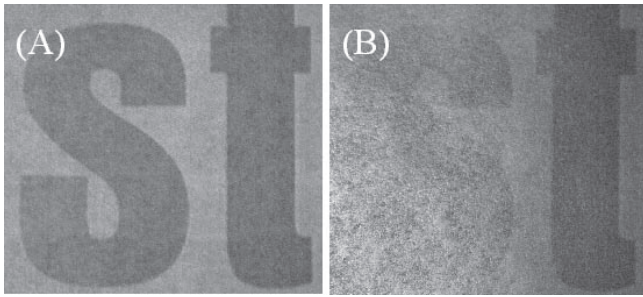


**Figure 1.** An electrophotographic image viewed under conditions of illumination that (A) show no gloss and (B) show gloss.

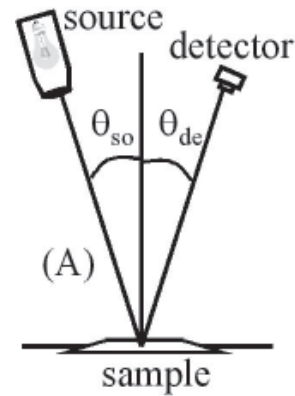


**Figure 2.** Illumination angle,  $\theta_{so}$ , and detection angle,  $\theta_{de}$ , are equal and opposite in most instruments designed to measure gloss.

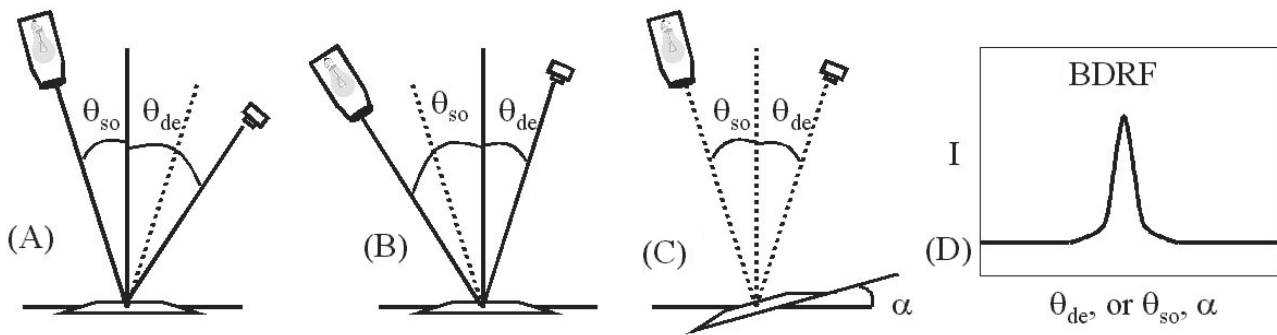


**Figure 3.** A goniophotometer measures reflected light as a function of (A) the angle of detection  $\theta_{de}$ ; (B) the angle of illumination  $\theta_{so}$ ; and/or (C) the angle of tilt of the sample,  $\alpha$ . Each produced a bi-directional reflectance factor function, BDRF, illustrated in (D).

regions, and between printed regions and the background paper, are often seen as objectionable. Several instrumental techniques have been reported recently for measuring gloss and gloss variations,<sup>7-10</sup> but a completely satisfactory analytical technique has not yet been shown to provide a high correlation with the visual perception of gloss.

### The Geometry of Gloss

Traditional gloss meters are designed to measure light reflected from a surface illuminated and measured at equal but opposite angles, as illustrated in Fig. 2. Many commercial gloss meters provide the ability to make measurements at equal/opposite angles ranging from 20° to 75°. For non-polarized light, gloss increases as the gloss angle increases, in accordance with Fresnell's laws. For this reason, high gloss materials are measured at small angles, e.g., 20°, and plain paper is generally measured at high angles, e.g., 75°.

If a perfect mirror is measured, then the instrument shown in Fig. 2 would provide all the information needed to characterize gloss. However, surface roughness is well known to play a major role in the angular distribution of specular light.<sup>11-13</sup> An increase in surface roughness generally results in reduced gloss, as observed visually. Instrumentally this is generally measured as an increase in the angular distribution of the specular light. Angular distribution can be measured with a goniophotometer,

as illustrated in Fig. 3. A goniophotometer is an instrument that measures reflected light as a function of angle of detection,  $\theta_{de}$ , angle of source illumination,  $\theta_{so}$ , or angle of tilt of the sample,  $\alpha$ , to produce a so called bi-directional reflectance function, BDRF. The BDRF is not a single function. The measured BDRF can differ for measurements made as a function of  $\theta_{de}$ ,  $\theta_{so}$ , or  $\alpha$ .<sup>11-13</sup> Although surface roughness generally increases the width of the BDRF peak and decreases the peak height, the detailed effects of roughness on the shape of the BDRF depend on all three angles,  $\theta_{de}$ ,  $\theta_{so}$ , and  $\alpha$ . It is not surprising that a simple gloss meter measurement, with a fixed equal/opposite angle, does not provide a good correlation with visual perception of gloss properties.

### A Micro-Goniophotometer

An instrument reported previously combined the spatial scanning capability of a microdensitometer with a goniophotometer by wrapping the sample around a cylinder, as illustrated in Fig. 4.<sup>8</sup> The sample is illuminated with collimated light, and an image can be captured with a camera sufficiently far from the sample to minimize parallax. Alternatively, a telecentric lens can be used.

The  $x$  direction of the image captured in Fig. 4 corresponds to changes in the tilt of the surface angle,  $\alpha$ , for fixed angles of illumination and detection,  $\theta_{de}$  and  $\theta_{so}$ . From the geometry of a circle, the horizontal location,

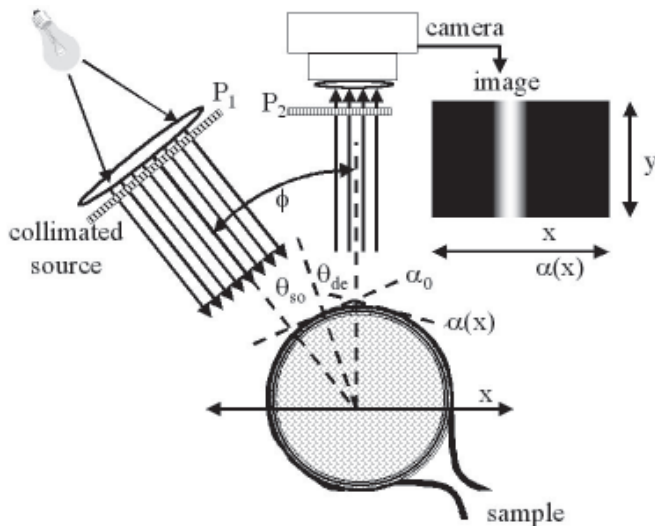


**Figure 4.** Cylindrical sample geometry of the micro-goniophotometer. The  $y$  direction is collinear with the axis of the cylinder, and the  $x$  direction is through the diameter of the cylinder.  $P_1$  and  $P_2$  are linear polarizing filters. This figure is not drawn to scale.

$x$ , can be converted into the mean tilt angle,  $\alpha$ , of the sample by Eq. (1), where  $r$  is the radius of the cylinder.

$$\alpha(x) = \sin^{-1}(x/r) \quad (1)$$

By scanning the  $x$  direction of the captured image, and by calibrating the camera to radiometric units, a BDRF can be generated for the sample. The BDRF generated in this way is a measure of surface irradiance,  $I$ , versus sample angle,  $\alpha$ , as illustrated in Fig. 3(C). By scanning in the  $y$  direction (co-linear with the axis of the cylinder), one can observe how the BDRF varies across the surface of the sample.

We define the angle of the surface as  $\alpha = 0$  at the point of maximum specular reflectance on the peak of the BDRF. Moving around the cylinder toward the light source is a surface tilt of  $\alpha > 0$ , and a tilt away from the source is  $\alpha < 0$ .

### Separating Specular from Diffuse Light

The term “diffuse light” often is used to describe the diffusion of gloss light over many angles, as shown by the width of the BDRF peak. The term is also used to describe light that penetrates the sample, scatters both spatially and angularly, and then returns to the surface as reflected light. In this report, the term “diffuse light” will be used to mean the latter, and the term “angularity distributed specular light” the former. The diffuse light is the component primarily responsible for the color in a printed sample, and specular light, primarily responsible for gloss effects, is distributed over many angles indicated by the width of the BDRF.

Experimentally, both specular light and diffuse light are reflected from a printed surface. To measure only the specular light, the diffuse light must be eliminated from the measurement. This is achieved in ordinary gloss meters by measuring only at the peak of the BDRF where specular light is concentrated and diffuse light is negligible by comparison. However, Fresnel’s laws tell us that if one measures the entire specular and diffuse

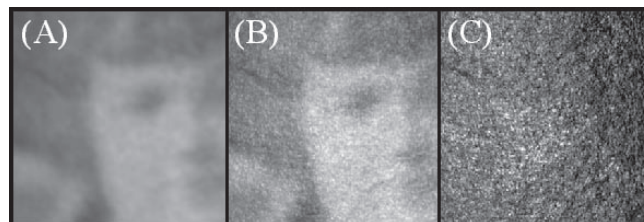


**Figure 5.** Images of a conventional AgX/gelatin print captured through a microscope (7 mm field of view) illuminated with a lamp located to produce gloss reflections primarily on the left side of the sample. Linear polarizers were used in front of the lamp and the camera. The polarizers were crossed in image (A) and aligned in image (B). Image (C) is the difference image.

components of reflected light, distributed over all angles, the specular component represents only about 4% of the total light. Therefore, BDRF measurements need to distinguish between specular and diffuse light in other ways. The technique applied in the current work is based on the polarization characteristics of Fresnel’s laws.<sup>9</sup> This is illustrated in Fig. 5.

The images in Figs. 5(A) and 5(B) are of a conventional silver halide, gelatin print captured with a CCD camera mounted on a microscope. The sample was illuminated with an incandescent lamp arranged to produce significant amounts of specular reflection on the left side of the print. Linear polarizers were placed in front of the lamp and the camera, as illustrated in Fig. 4,  $P_1$  and  $P_2$ . When these polarizers are aligned in the same direction of polarization, both specular and diffuse light are observed, as illustrated in Fig. 5(B). However, if the polarizing filter in front of the camera is rotated 90°, the specular light is blocked, resulting in Fig. 5(A). The specular light maintains polarization, but diffuse light does not. Thus, for a camera of gamma 1.0 (pixel value proportional to irradiance) the specular component is the difference between the images as shown in Fig. 5(C). The distribution of specular light is an indicator of surface roughness.<sup>8,9</sup>

The polarization technique is used in this instrument to define the specular component of the light. For  $\theta_o = \theta_i = 20^\circ$ , measurements made with both orthogonal directions of polarization ( $p$  and  $s$ ) behaved indistinguishably.

### Measurements of the BDRF

The capabilities of the instrument shown in Fig. 4 were examined by making a series of measurements on a variety of materials. For example, Fig. 6 shows measurements made on a plain paper, a highly calendered paper, and a sheet of aluminum foil. As one would expect, the height of the BDRF peak correlates with the very different levels of visual gloss of these three samples.

To further examine the utility of the micro-goniophotometer of Fig. 4, measurements were made on a series of old silver/gelatin prints from a family album. The prints represented a range of visual levels of gloss. Measurements of both the BDRF peak height,  $h$ , and a traditional 20° gloss number were made. The gloss meter used in this experiment was a Gardner gloss meter calibrated against a black glass. The gloss meter readings are shown versus the BDRF peak heights,  $h$ , in Fig. 7. Unlike the gloss meter measurements, the BDRF measurements are not calibrated to a black glass. Rather, the peak heights are shown relative to the highest value observed.

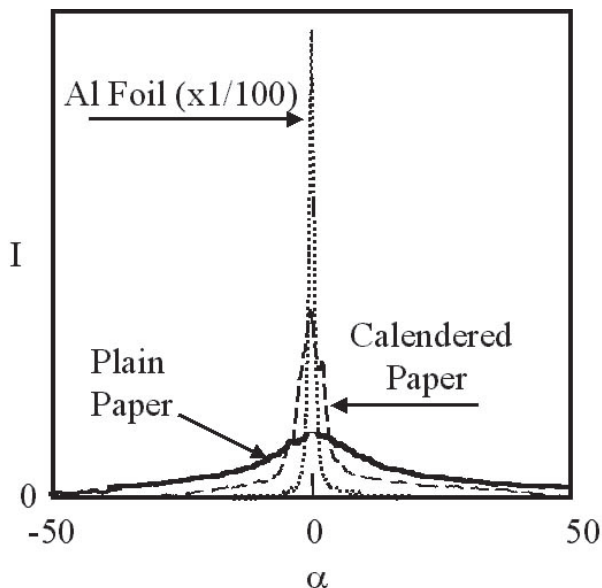


**Figure 6.** BDRFs for three materials representing very different gloss levels. Measurements were made with the instrument in Fig. 4 using a point source illuminator. Aluminum foil was measured with 1/100th illumination power in order to keep the camera pixel values on scale.

The results in Fig. 7 are typical for comparing gloss from different instruments. The correlation is clearly evident, but it is not very high. Multiple measurements made with both the gloss meter and the micro-goniophotometer were made on several of the samples, and estimates of the  $2\sigma$  error bars were made for each instrument, as indicated by the error bars illustrated Fig. 7. It is clear that the poor correlation between the two instruments is not a result of experimental uncertainty with either instrument. Rather, the low correlation indicates that the instruments are measuring slightly different properties of specularly reflected light. It is no wonder that traditional gloss measurements provide only limited correlations with visual gloss.

In order to investigate the micro-goniophotometer further, measurements were made on a series of substrates commonly used in inkjet and electrophotographic printing. Measurements were made with a point source illuminator, and both the area of the BDRF,  $A$ , and the height of the BDRF,  $h$ , were measured. Figure 8 shows  $A$  versus  $h$ .

The printing substrates used in this experiment fell into three groups, plain paper, a calendered sheet, and synthetic plastic sheets. Measurement of both  $A$  and  $h$  provides more information than a single measurement of  $h$  or of instrumental gloss, and it is easy to segment these different types of sheets. However, this is not an impressive accomplishment, and the reason for the differences among the members of the three groups remains obscure. That is, it is not possible from this data to distinguish between effects of surface roughness and effects of different material properties such as the index of refraction. An additional modification to the micro-goniophotometer, described below, enables this distinction to be made.

#### The Other Tilt Angle

Surface roughness is well known to influence the shape of the BDRF. The tilt angle described in Fig. 4 is the over-

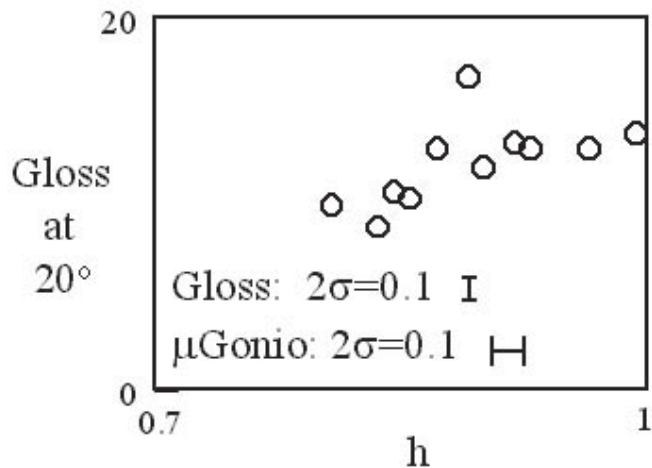


**Figure 7.** Gloss meter value measured at  $20^\circ$  specular angle versus peak height of the BDRF measured with the instrument illustrated in Fig. 4. Error bars and values of  $2\sigma$  are estimated from multiple measurements of several samples.

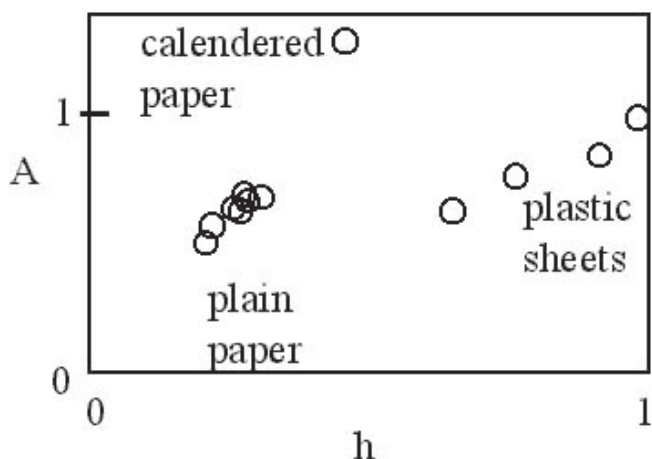


**Figure 8.** Area of the BDRF,  $A$ , versus the height of the BDRF peak,  $h$ , commonly encountered printing substrates.

all mean angle,  $\alpha$ , and microscopic surface roughness can be described as a random variation in this angle,  $\sigma_\alpha$ . The entire BDRF of the sample is a function not only of the angle  $\alpha$ , but also of the orthogonal angle  $\beta$ . Surface roughness is a random variation in both directions,  $\sigma_\alpha$  and  $\sigma_\beta$ . The peak of the BDRF occurs where both of the mean surface angles are  $\alpha = \beta = 0$ . Surface roughness broadens the BDRF in both the  $\alpha$  and the  $\beta$  directions from the peak. If the index of refraction of the sample does not change, then a change in roughness would be expected to change only the width and height of the two dimensional BDRF. The volume of the BDRF should remain constant. The volume of the BDRF then represents the total amount of specular light reflected in accordance with Fresnel's laws, and the total amount of specularly reflected light should be a function of the index of refraction of the materials in the image.

It would be useful to measure both the peak height and the total volume of the two dimensional BDRF. However, a BDRF measured versus both  $\alpha$  and  $\beta$  is not achievable with the instrument shown in Fig. 4. To overcome this difficulty, the instrument was designed to collect all of the gloss light in the  $\beta$  direction. This is done

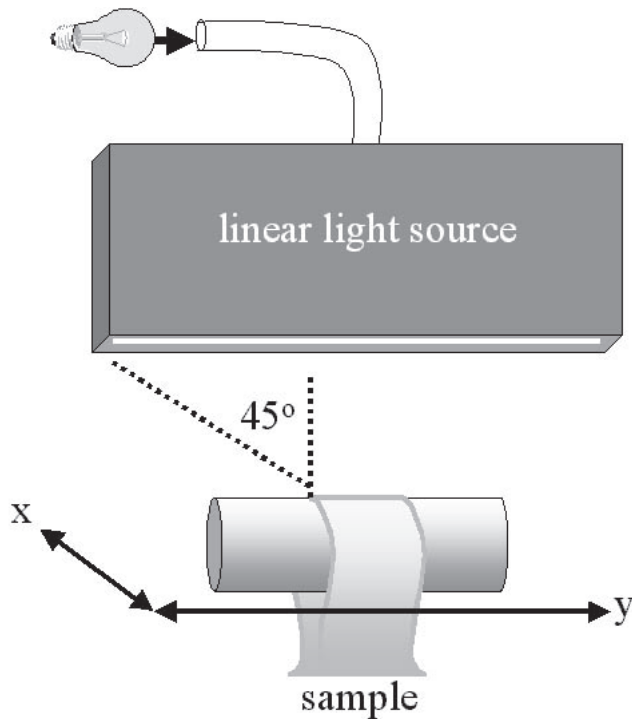


**Figure 9.** Micro-goniophotometer geometry with a linear fiber optic illuminator. The  $x$  and  $y$  directions are the same as shown in Fig. 4, with the  $x$  direction orthogonal to the plane of the diagram. The detector is in the  $x,z$  plane orthogonal to the plane of the diagram.

by using the long, thin illuminator shown schematically in Fig. 9.

The linear light source illustrated in Fig. 9 is co-linear with the sample cylinder. In the current instrument, the linear source is long enough so that a micro-facet on the sample may be tilted in the  $\beta$  direction by as much as  $45^\circ/2$  from the mean surface and still direct specular light into the camera. This is analogous to using a long, thin slit in traditional microdensitometry. Irradiance is averaged in one dimension ( $\beta$  in this case) and scanned in the other dimension,  $\alpha$ . An ideal instrument would use an infinitely long source in order to guarantee capturing all of the  $\beta$  direction gloss, but the system shown in Fig. 6 was used as an approximation of the ideal instrument. If this approximation is a useful one, then the area under the two-dimensional BDRF curve ( $I$  versus  $\alpha$ ) should be proportional to the total specular light reflected from the object, and therefore should depend only on Fresnel's laws and the index of refraction of the material. In other words, samples composed of the same material but with different levels of surface roughness should have the same area,  $A$ , under the BDRF but different peak heights,  $h$ .

### Testing the Instrument

The geometry shown in Fig. 4 with linear illumination as shown in Fig. 9, defines the final microgoniophotometric instrument developed in this project. The source-to-camera angle was set at  $\phi = 40^\circ$ , so the instrument measures the BDRF for  $20^\circ$  illumination/detection. Measurements described below were made with  $s$  polarized light, but at  $20^\circ$  no experimentally significant differences were observed between  $s$  and  $p$  polarization.

In order to test whether the area under the measured BDRF,  $A$ , is constant for samples of the same material

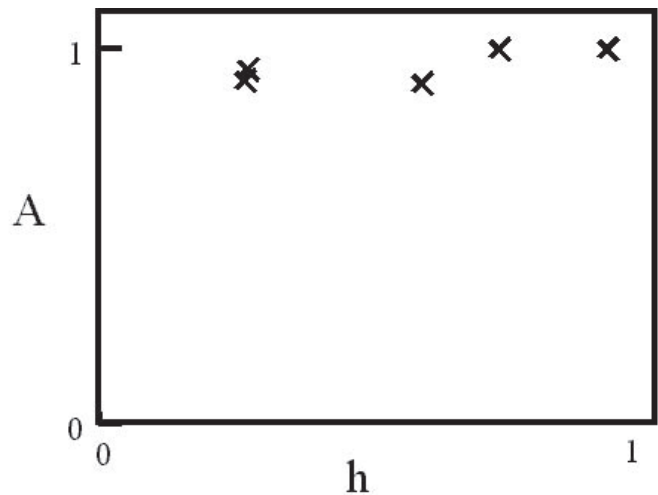


**Figure 10.** Area,  $A$ , versus height,  $h$ , for BDRF measurements on aluminum samples buffed to different levels of roughness.  $A$  and  $h$  normalized to the sample with the highest  $h$ .

at different levels of roughness, measurements were made on samples of aluminum foil. The foil samples were buffed to varying degrees with a rough piece of paper and fine steel wool to generate different degrees of visual gloss and surface roughness. The BDRF of each sample was measured using the linear illuminator of Fig. 9, and values of  $h$  and  $A$  were extracted from each BDRF. Figure 10 shows the results, and it is evident that indeed the BDRF area is approximately constant for a wide range of peak heights.

The printing substrates examined in Fig. 8 were re-measured with the micro-goniophotometer using the linear illuminator as shown in Fig. 9. Additional samples of calendared and coated sheets commonly used in offset printing were also measured. Values of  $A$  and  $h$  were extracted from each BDRF measurement, and the results are shown in Fig. 11.

The results shown in Fig. 11 indicate that the large range of instrumental gloss values,  $h$ , observed with the plastic sheets can be attributed to differences in roughness rather than differences in a material property such as refractive index. Similarly, the coated and calendared sheets show a wide range of gloss,  $h$ , attributable primarily to roughness differences. However, as a group the plastic sheets appear to have indices of refraction that are lower than the coated and calendared sheets. The plain papers show an approximate proportionality between  $A$  and  $h$ . However, the variation in  $A$  with  $h$  is an experimental artifact of the finite linear illuminator. As shown in Fig. 6, the BDRF of plain paper is significantly broader than the  $\pm 22.5^\circ$  covered by the linear illuminator. Thus, the approximation of an infinitely long illuminator is not a good approximation for the plain papers. The instrument in its current configuration is useful only for making measurements on relatively high gloss samples. A longer linear illuminator is needed for measurements on plain paper.

A final test of the instrument is illustrated by the BDRFs shown in Fig. 12. In this experiment, samples of a calendared printing substrate were printed with solid patches of ink on a commercial press using liquid electrophotography (Indigo UltraStream). Values of area,  $A$ , and height,  $h$ , are shown relative to the calendared sheet.

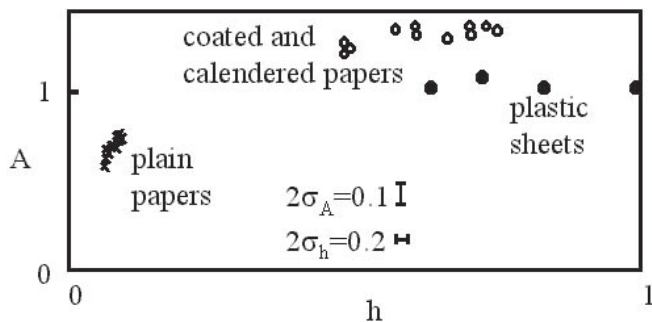


**Figure 11.** Area,  $A$ , versus height,  $h$ , for BDRF measurements on printing substrates.  $A$  and  $h$  normalized to the sample with the highest  $h$ .

The printed samples all appeared more glossy than the unprinted paper, and this is consistent with the higher values of  $h$ . However, the BDRF areas,  $A$ , are lower than observed for the unprinted paper. This indicates the inked samples have optical material properties that are significantly different from the unprinted paper. Moreover, the progressive change in the shapes of the BDRFs appears to indicate a progressive smoothing of the ink surface as more ink is added to the substrate.

### Conclusion

When used with a linear illuminator, the instrument shown schematically in Fig. 4 is capable of providing significantly more information about specularly reflected light than can be obtained with a conventional gloss meter. However, the measurement does not require significantly greater effort. A sample is mounted on the cylindrical sample holder, and images are captured with orthogonal directions of one polarizing filter. The two images are processed to return values of  $A$  and  $h$  and plots the BDRF. The value of  $A$  provides information about the material optical properties of the system, and the shape of the BDRF indicates the nature of the roughness of the sample. This technique has a significant advantage over traditional gloss meters in that it accounts for all of the gloss light reflected from the surface, and it does so in a way that can be resolved spatially. The angular and spatial range over which measurements are made can be changed by changing the radius of the sample cylinder and the focal length of the camera lens. Thus, it is anticipated that measurements of this kind can be expected to yield useful correlates with visual gloss and also show useful information about the mechanisms of specular and diffuse reflection on printed samples. ▲

**Acknowledgment.** This project was sponsored by a grant from the Hewlett-Packard Corporation, with guidance from Norm Burningham and Ken Lindblom. Special thanks to Bob Chin, Manager of Digital Technologies in OMNOVA Solutions, Inc., for sponsorship of summer research support for undergraduate student participation in the project.

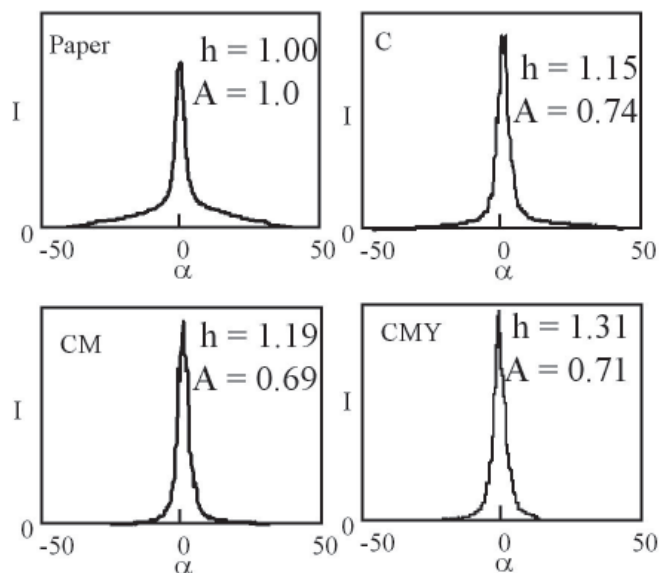


**Figure 12.** BDRFs for a calendered paper and the paper printed with cyan, cyan + magenta, and cyan + magenta + yellow. Measurements were made with the linear illuminator.

### References

1. P. C. Swanton and E. N. Dalal, Gloss preferences for color xerographic prints, *J. Imaging Sci. Technol.* **40** 2, 158 (1996).
2. J. A. Ferwerda, F. Pellacini and D. P. Greenberg, Psychophysically based model of surface gloss perception, *Proc. SPIE* **4299**, 291–301 (2001).
3. C. Kuo, Y. Ng and C. J. Wang, Gloss patch selection based on support vector regression, *IS&T's PICS Conference*, IS&T, Springfield, VA, 2002, pp. 121–125.
4. C. Kuo, Y. Ng and C. J. Wang, Differential gloss visual threshold under normal viewing conditions, *IS&T's NIP-18, International Conference on Digital Printing Technologies*, IS&T, Springfield, VA, 2002, pp. 467–470.
5. C. J. Wang, Differential gloss in electrophotography, *IS&T's NIP-17, International Conference on Digital Printing Technologies*, IS&T, Springfield, VA, 2001 pp. 406–407.
6. Y. S. Ng and J. Wang, Gloss uniformity attributes for reflection images, *IS&T's NIP-17, International Conference on Digital Printing Technologies*, IS&T, Springfield, VA, 2001, pp. 718–722.
7. P. Mehta, K. Johnson and D. Wolin, A new method of measuring gloss mottle and micro-gloss, *IS&T's NIP-17, International Conference on Digital Printing Technologies*, IS&T, Springfield, VA, 2001, pp. 714–717.
8. J. S. Arney and H. Tran, An inexpensive micro-goniophotometry you can build, *IS&T's PICS Conference Proc.*, IS&T, Springfield, VA, 2002, pp. 179–182.
9. J. S. Arney, K. Pollmeier and J. Michel, Technique for analysis of surface topography of photographic prints by spatial analysis of first surface reflectance, *J. Imaging Sci. Technol.* **46**(4), 350 (2002).
10. M. A. MacGregor and P. A. Johansson, Submillimeter gloss variations in coated paper: Part 1: The gloss imaging equipment and analytical techniques, *Tappi J.* **73**, 161 (1990).
11. M.-C. Beland and P. J. Mangin, *Surface Analysis of Paper*, T. E. Connors and S. Banerjee, Eds., CRC Press, Boca Raton, Florida, 1995, Chap. 1.
12. P. Wågberg and P. Johansson, Surface Profilometry: a comparison between optical and mechanical sensing on printing papers, *TAPPI J.* **76**, 115 (1993).
13. J. M. Bennett and L. Mattsson, *Introduction to Surface Roughness and Scattering*, 2nd ed., Optical Soc. of America, Washington, DC, 1999, Chap. 3.